THE JOURNAL OF COMPARATIVE NEUROLOGY 496:668–683 (2006)

Organization of Noradrenergic Efferents to Arousal-Related Basal Forebrain Structures

RODRIGO A. ESPAÑA AND CRAIG W. BERRIDGE*
Psychology Department, University of Wisconsin, Madison, Wisconsin 53706

ABSTRACT

Norepinephrine acts within select basal forebrain regions to modulate behavioral state and/or state-dependent processes, including the general regions encompassing the medial septal area, the medial preoptic area, and the substantia innominata. The present study examined the origin and organization of noradrenergic efferents to these basal forebrain regions by using combined immunohistochemical identification of noradrenergic neurons with retrograde tracing. Results indicate that the locus coeruleus provides the majority of noradrenergic input to these regions. Lesser, although at times substantial, contributions from the A1/C1 and A2/C2 adrenergic cell groups were also observed, particularly in the case of the medial preoptic region. Given the prominent state-modulating actions of the locus coeruleus, additional studies examined: 1) lateralization of locus coeruleus efferents to these regions; 2) the topographical organization of basal forebrain-projecting locus coeruleus neurons; and 3) the degree of collateralization of individual locus coeruleus neurons across these regions. Approximately 80–85% of locus coeruleus efferents to these regions project ipsilaterally. In general, basal forebrain-projecting neurons were distributed throughout the entire dorsoventral and rostrocaudal extent of the locus coeruleus. Additionally, a large proportion of locus coeruleus neurons project simultaneously to these basal forebrain terminal fields. Combined, these observations indicate coordinated actions of locus coeruleus neurons across these basal forebrain regions implicated in the regulation of behavioral state and/or state-dependent processes. J. Comp. Neurol. 496:668–683, 2006.

Indexing terms: locus coeruleus; medial preoptic area; medial septum; norepinephrine; retrograde tract tracing; substantia innominata

The locus coeruleus (LC) is a small pontine nucleus that through an extensive efferent projection system provides the majority of forebrain norepinephrine (NE). Extensive evidence indicates that the LC-noradrenergic system exerts potent modulatory actions on forebrain neuronal and behavioral activity states (for review, see Berridge and Waterhouse, 2003). For example, LC neurons display state-dependent discharge rates, such that they are more active in waking than in sleep (Hobson et al., 1975; Foote et al., 1980; Aston-Jones and Bloom, 1981). Consistent with this, unilateral enhancement of LC neuronal discharge rates elicits robust bilateral activation of the forebrain as measured by electroencephalographic (EEG) activity in the halothane-anesthetized rat (Berridge and Foote, 1991). Conversely, bilateral suppression of LC discharge activity increases EEG indices of sedation in the lightly anesthetized rat (Berridge et al., 1993).

Additional studies indicate that noradrenergic efferents act within an extended region of the medial basal forebrain to modulate behavioral state. This region encompasses the general region of the medial septal area (MSA; including the medial septum and the diagonal band of Broca) and the general region of the medial preoptic area (MPOR; including the medial preoptic area proper and the medial preoptic nucleus). Infusion of NE or noradrenergic α_1- or β-receptor agonists into either of these regions increases EEG and behavioral indices of alert waking (Ber-

Grant Sponsor: The University of Wisconsin Graduate School; Grant number: PHS DA10681; Grant number: DA00389; Grant number: MH62359.

*Correspondence to: Craig W. Berridge, Psychology Department, University of Wisconsin, 1202 W. Johnson St., Madison, WI 53706-1611. E-mail: berridge@wisc.edu

Received 17 May 2005; Revised 4 August 2005; Accepted 20 December 2005

DOI 10.1002/cne.20946

Published online in Wiley InterScience (www.interscience.wiley.com).

ridge and Foote, 1996; Berridge et al., 1996, 2003; Berridge and O'Neill, 2001). In contrast, infusions placed immediately outside these regions do not alter behavioral state. The substantia innominata (SI) plays a prominent role in the regulation of EEG activity state (Buzsaki et al., 1988; Metherate et al., 1992), and NE modulates SI neuronal activity (Fort et al., 1995). Thus, it is interesting that NE, amphetamine, or noradrenergic receptor agonists infused into the SI do not alter EEG or behavioral indices of arousal (Berridge et al., 1999; Berridge and O'Neill, 2001). The only exception to this is observed following high doses of NE (Cape and Jones, 1998; Berridge and O'Neill, 2001). Thus, the MSA and MPOR appear to differ from the SI in terms of sensitivity to the wake-promoting actions of NE. This is in contrast to that observed with hypocretin (orexin), which exerts wake-promoting actions when infused into the MSA, MPOR, or SI (España et al., 2001; Thakkar et al., 2001).

The above-described observations indicate a prominent role of NE within a circumscribed region of the medial basal forebrain in the regulation of behavioral state and state-dependent processes. To date, much remains unknown concerning the origin and organization of noradrenergic efferents to basal forebrain arousal-related regions. Previous studies demonstrate that all three of these basal forebrain regions receive noradrenergic input from the LC (Segal and Landis, 1974; Jones and Moore, 1977; Moore, 1978; Krayniak et al., 1981; Zaborsky, 1989). Nonetheless, a number of important questions remain concerning the organization of noradrenergic efferents to basal forebrain regions associated with the regulation of behavioral state. First, the proportion of noradrenergic innervation of the MSA, MPOR, and SI that originates from the LC vs. other noradrenergic nuclei remains unknown. For example, in the case of the shell subdivision of the nucleus accumbens and the ventrolateral preoptic area (VLPO), these basal forebrain structures receive the majority of noradrenergic input from noradrenergic nuclei other than the LC (Delfs et al., 1998; Chou et al., 2002).

Second, the LC projects to the neocortex in a predominantly ipsilateral manner, whereas the degree of lateralization to subcortical regions varies depending on the terminal field (Simpson et al., 1997). The degree to which the noradrenergic innervation of basal forebrain arousal-related structures is lateralized has not been well characterized. Third, extensive evidence indicates a general topographic organization of LC neurons projecting to cortical and subcortical sensory systems (Segal and Landis, 1974; Loy et al., 1980; Haring and Davis, 1983; Waterhouse et al., 1983, 1993). For example, cortically projecting neurons tend to be located caudally within the LC (Waterhouse et al., 1983). Moreover, across cortical fields, cortically projecting LC neurons display a differential distribution within the LC in both the dorsoventral and rostrocaudal dimensions (Waterhouse et al., 1983). The extent to which LC neurons projecting to basal forebrain arousal-related structures are topographically organized is currently not known.

Finally, it has been demonstrated previously that subsets of individual LC neurons project to functionally related structures (e.g., cortical, thalamic, and brainstem somatosensory nuclei; Simpson et al., 1997). However, the extent to which individual LC neurons simultaneously target the MSA, MPOR, and/or SI is not known. Given the differential sensitivity to the wake-promoting actions of NE across the MSA and MPOR vs. SI, it is of interest to determine whether there are corresponding differences in the origin and/or organization of noradrenergic efferents across these basal forebrain regions.

The current studies utilized single and double retrograde labeling of noradrenergic neurons to characterize better the anatomical organization of noradrenergic efferents to basal forebrain structures associated with the regulation of behavioral state. Single retrograde tracing using Fluoro-Gold (FG) or cholera toxin B subunit (CTb), combined with immunohistochemical visualization of dopamine-β-hydroxylase (DBH), the NE synthetic enzyme, demonstrated that the LC is the primary source of noradrenergic innervation to these three basal forebrain regions. Based on these observations, additional analyses examined the degree to which LC neurons projecting to these regions are lateralized and topographically organized. Finally, in a subset of cases, dual infusions of FG and CTb were used to examine the extent to which individual LC neurons collateralize to multiple arousal-related basal forebrain terminal fields. In these latter studies, animals received a pair of tracer infusions into different basal forebrain noradrenergic terminal fields (e.g., FG into the MSA and CTb into the MPOR). The degree to which individual LC neurons were labeled by both tracers was then measured.

Abbreviations

ACB	nucleus accumbens
aco	anterior commissure
BST	bed nucleus of the stria terminalis
C	central canal
DBH	dopamine β-hydroxylase
DTN	dorsal tegmental nucleus
FG	Fluoro-Gold
fx	fornix
int	internal capsule
LC	locus coeruleus
LPO	lateral preoptic area
LRN	lateral reticular nucleus
LS	lateral septum
MA	magnocellular preoptic area
MEV	mesencephalic nucleus of the trigeminal
MPN	medial preoptic nucleus
MPO	medial preoptic area
MPOR	medial preoptic area
MS	medial septum
MSA	medial septal area
NDB	nucleus of the diagonal band of Broca
NI	nucleus incertus
och	optic chiasm
PB	parabrachial nucleus
scp	superior cerebellar peduncle
SI	substantia innominata
SLC	subcoeruleus nucleus
SubC	subcoeruleus nucleus
VL	lateral ventricle
VLPO	ventrolateral preoptic area
V3	third ventricle
V4	fourth ventricle

MATERIALS AND METHODS

Animals

Adult male Sprague-Dawley rats (300–400 g, Sasco, Oregon, WI) were housed in pairs for at least 14 days prior to surgery with ad libitum access to food and water on an 13/11-hour light/dark cycle (lights on 7:00 am).

Surgery

All animals were anesthetized by using halothane and then placed in a stereotaxic instrument with the incisor bar set at −11.5 mm below ear bar zero. Retrograde tracer infusions were made into the MSA (−0.75 A, 1.5L, −6.7V), MPOR (−2.0A, 1.8L, −7.6V), and/or SI (−1.9A, 3.4L, −7.6V) using glass pipettes (see below). Infusion pipettes were inserted at an angle of 4° from vertical. In all cases, an incision was made in the dura mater with a 30-gauge needle prior to insertion of the infusion pipette. At the end of surgery, all animals received buprenorphine (0.01 mg/kg; Reckett Beckiser Pharmaceutical, Richmond, VA) and penicillin (300,000 U/ml; G.C. Handford, Syracuse, NY). All facilities and procedures were in accordance with the guidelines regarding animal use and care put forth by the National Institutes of Health of the United States and were supervised and approved by the Institutional Animal Care and Use Committee of the University of Wisconsin.

Infusion procedures

FG (Fluorochrome, Denver, CO) or CTb (List Biological Laboratories, Campbell, CA) were used as retrograde tracers to identify noradrenergic efferents to the MSA, MPOR, or SI. For FG, single-barrel glass micropipettes (15–25 μm diameter; Friedrich and Dimmock, Millville, NJ) were filled with 2% FG solution (dissolved in saline) as previously described (Valentino et al., 1994). Once the infusion pipette was positioned at the appropriate coordinates (see above), FG was iontophoresed (5.0 μA, 15 minutes, 5-second pulses, 50% duty cycle), and the pipette was left in place for 10 minutes. For infusions of CTb, single-barrel glass micropipettes (20–30 μm diameter; Friedrich and Dimmock) were filled with 1% CTb solution as described previously (Valentino et al., 1994). CTb was ejected by applying small pulses of pressure (40–80 psi, 50–100 msec duration) to the calibrated pipette (60 nl/mm). Approximately 200–300 nl of solution was ejected over a period of at least 10 minutes, and the pipette was left in place for an additional 10 minutes. For both FG and CTb infusions, animals were sacrificed 7 days following surgery and infusion.

To examine collateralization of LC efferents to basal forebrain structures, an infusion of FG was made into the MSA, MPOR, or SI, and a CTb infusion was made into one of the two remaining basal forebrain regions within the same animal, as described above. For all animals tested, combinations of retrograde tracer infusions were made into the same hemisphere (e.g., FG into the left MSA and CTb into the left MPOR). Animals were sacrificed 7 days following the infusions to ensure optimal retrograde distribution of tracer (Valentino et al., 1994).

Histology and immunohistochemistry

All animals were deeply anesthetized with sodium pentobarbital (Abbott Laboratories, North Chicago, IL) and perfused transcardially with 250 ml heparinized saline (1 unit of heparin/ml 0.9% saline; heparin was obtained from SoloPak Laboratories, Elk Grove Village, IL) followed by 400 ml of 4% paraformaldehyde in 0.01 M phosphate buffer (pH 7.4). Brains were removed, stored in paraformaldehyde overnight, and taken through graded sucrose solutions (10-20-30% sucrose in 0.01 M phosphate buffer, pH 7.4). A tracking mark was made in the right lateral cortex and brainstem, and 40-μm-thick sections were collected into six series (wells) by using a cryostat. Therefore, sections within any single well were separated by 200 μm (i.e., 5 × 40 μm). Sections were then placed in 0.01 M phosphate-buffered saline (PBS; pH 7.4) with 0.1% sodium azide and stored at 4°C.

For immunohistochemical processing of FG, sections were rinsed with 0.01 M PBS and then incubated for 20 minutes in a quench solution containing 0.75% hydrogen peroxide. Sections were then rinsed and incubated for 48 hours at 4°C with rabbit anti-FG antibody (1:2,000; Chemicon, Temecula, CA; cat. no. AB153) diluted in 0.01 M/PBS containing 0.1% Triton-X-100 (PBS-TX; Sigma Chemical Co., St. Louis, MO). After incubation, tissue was rinsed with 0.01 M PBS-TX and incubated with donkey-anti-rabbit antibody (1:500; Jackson ImmunoResearch, West Grove, PA) for 90 inutes. Tissue was then rinsed with 0.01 M PBS-TX, exposed to rabbit peroxidase anti-peroxidase (PAP; 1:500; Dako, Carpinteria, CA) for 90 minutes, and rinsed with 0.01 M PBS-TX. Sections were reacted with diaminobenzidene (DAB; Vector, Burlingame, CA) to yield a brown precipitate.

For immunohistochemical processing of CTb, sections were rinsed with 0.01 M PBS and then incubated for 20 minutes in a quench solution containing 0.75% hydrogen peroxide. Sections were then rinsed and incubated for 48 hours at 4°C with goat anti-CTb antibody (1:40,000; Accurate Chemical and Scientific, Westbury, NY; cat. no. 703) diluted in 0.01 M PBS-TX. After incubation, tissue was rinsed with 0.01 M PBS-TX and incubated with donkey-anti-goat antibody (1:500; Jackson ImmunoResearch) for 90 minutes. Tissue was then rinsed with 0.01 M PBS-TX, exposed to ABC (1:500; Vector) for 90-minutes, and rinsed with 0.01 M PBS-TX. Sections were reacted with DAB (Vector) to yield a brown precipitate.

For dual visualization of FG and DBH, or CTb and DBH (FG + DBH or CTb + DBH), sections were first stained for FG or CTb as described above and then incubated for 48 hours at 4°C with mouse anti-DBH antibody raised against purified bovine DBH (1:1,000,000 for LC sections, 1:200,000 for all other brainstem sections; Chemicon; cat. no. MAB308) diluted in 0.01 M PBS-TX. The distribution of DBH-ir neurons obtained from this antibody was identical to that described previously (Lindvall and Bjorklund, 1983; Saper et al., 1983; Tucker et al., 1987). After incubation, tissue was rinsed with 0.01 M PBS-TX and incubated with donkey-anti-mouse antibody (1:500; Jackson ImmunoResearch) for 90 minutes. Tissue was then rinsed with 0.01 M PBS-TX, exposed to ABC (1:500; Vector) for 90 minutes, and rinsed with 0.01 M PBS-TX. Sections were reacted with SG blue to yield a blue precipitate (Vector). This sequence of staining allowed for optimal discrimination of single- (FG, CTb, or DBH) versus double-labeled cells (FG + DBH or CTb + DBH) and did not appear to alter the staining quality or the average cell counts commonly observed when individual labeling for FG, CTb, or DBH was used.

When FG and CTb were visualized within the same tissue section, sections were first stained for CTb (brown

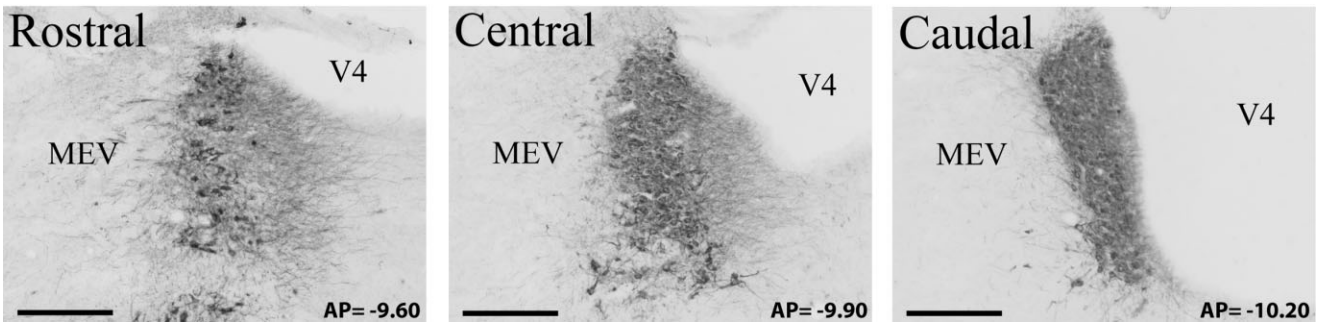

Fig. 1. Photomicrographs depicting the rostrocaudal extent of DBH-ir neurons within the LC nucleus. The LC nucleus was divided into these three rostrocaudal levels for topographical analyses (see Materials and Methods). AP numbers refer to approximate coronal level relative to bregma. For abbreviations, see list. Scale bar = 300 μm.

reaction product) followed by staining for FG (blue reaction product; Vector). This sequence of staining allowed for optimal discrimination of single- (FG or CTb) versus double-labeled cells (FG + CTb) and did not appear to alter the staining quality or the average cell counts commonly observed when individual labeling for FG or CTb was used. In all cases, omission of the primary antibody resulted in the absence of labeling within tissue.

Our immunoperoxidase-based analyses indicated double labeling (DBH + retrograde label) largely within the LC, A1, and A2 only. To ensure the reliability of immunoperoxidase-based analyses of single and double labeling within these regions, FG and DBH were also visualized by using immunofluorescence. For these cases, sections were first incubated for 48 hours at 4°C with rabbit anti-FG antibody (1:2,000; Chemicon; cat. no. AB153) diluted in 0.01 M PBS-TX. After incubation, tissue was rinsed with 0.01 M PBS-TX and incubated with a Cy3-conjugated donkey-anti-rabbit antibody (1:500; Jackson ImmunoResearch) for 90 minutes and then rinsed. After FG processing, tissue was incubated for 48 hours at 4°C with mouse anti-DBH antibody (1:500,000; Chemicon; cat. no. MAB308) diluted in 0.01 M PBS-TX. After incubation, tissue was rinsed with 0.01 M PBS-TX and incubated in fluorescein-conjugated rabbit anti-mouse antibody (1:500; Jackson ImmunoResearch) for 90 minutes.

Sections processed with immunoperoxidase techniques were mounted on microscope slides (Fisher Scientific, Itasca, Il), air-dried, dehydrated in graded alcohols (50–100%), cleared for 24 hours (Histoclear; Fisher Scientific), and coverslipped by using DPX mounting medium (BDH Laboratory Supplies, Garden City, NY). Sections processed for immunofluorescence were mounted on microscope slides (Fisher Scientific), air-dried, and coverslipped with Prolong mounting medium (Molecular Probes, Eugene, OR).

Data analyses and photomicrograph production

For each region, the absolute numbers of DBH-ir, retrogradely labeled, and double-labeled neurons was counted by using an Olympus BX51 light and reflected immunofluorescence microscope. For examination of retrogradely labeled DBH neurons within the A1/C1, A2/C2, A4, A5, LC (A6), A7, subcoeruleus (SLC) and C3, single- (FG, CTb, or DBH), or double- (FG+DBH or CTb+DBH) labeled neurons were counted from both hemispheres in each animal, and analyses encompassed the full rostrocaudal extent of each of these noradrenergic/adrenergic regions (nonadjacent sections, see above). The vast majority (90–95%) of immunoreactive cells that were counted as "DBH-ir neurons" possessed a clearly definable nucleus whose diameter fell within a range of 8–10 μm depending on the noradrenergic/adrenergic region examined. In the few cases in which there was a distinct cell profile but no nucleus visible (often due to the dense DBH staining observed in the LC), immunoreactive cells were counted as "DBH-ir neurons" only when they were largely spherical in shape and had a diameter comparable to, or greater than, the average size of DBH-ir nuclei.

For immunoperoxidase-processed tissue, cells were considered double-labeled only when 1) obvious areas of DAB (brown) and SG blue (blue) precipitate were observed in a heterogeneous fashion within the same cell; or 2) DAB brown and SG blue precipitate overlapped in a relatively homogenous fashion to produce a dark gray-brown color clearly distinct from either DAB or SG blue single-labeled cells. Within the LC, in some cases retrogradely labeled cells were often darkly stained, making discrimination between brown and blue somewhat difficult. In these cases, DBH immunoreactivity within processes clearly extending from the soma could often be used as an indicator of double labeling. In all cases, a cell was counted as double-labeled only when evidence of both brown and blue precipitates was visible in that cell. For immunofluorescent tissue, cells were considered double-labeled only when fluorescence was clearly observed for both FG (red fluorescent signal) and DBH (green fluorescent signal) within the same cell. Cell counts were adjusted by obtaining a random sampling of the nuclear diameters for neurons located within each noradrenergic/adrenergic region and then applying Abercrombie's correction factor (Abercrombie and Johnson, 1946) to get an accurate estimation of the actual number of cells present per section examined.

For the LC, counting of labeled neurons was initiated at the rostralmost pole of the LC (~AP = −9.00, relative to Bregma) and continued through the caudalmost portions of the LC (~AP = −10.30). On average, counting was conducted on eight to nine sections per animal and in all cases, at least one rostral (~AP = −9.60), one central (~AP = −9.85), and one caudal (~AP = −10.10) DBH-rich section was utilized for these analyses (Fig. 1).

In the case of other noradrenergic/adrenergic regions, counting began at the first sign of consistent DBH immunoreactivity, within a particular structure, and continued until no more DBH-ir neurons were observed in that structure. For the A1/C1, DBH-ir neurons were commonly observed at (~AP = −11.90) through (~AP = −16.10) and on average, spanned 14–17 sections per animal. For the A2/C2, DBH-ir neurons were commonly observed at (~AP = −11.90) through (~AP = −16.90) and spanned 14–17 sections per animal. For the A4, DBH-ir neurons were commonly observed at (~AP = −10.30) through (~AP = −11.30) and spanned five to six sections per animal. For the A5, DBH-ir neurons were commonly observed at (~AP = −9.50) through (~AP = −11.00) and spanned 11–13 sections per animal. For the A7, DBH-ir neurons were commonly observed at (~AP = −8.80) through (~AP = −9.20) and spanned two to three sections per animal. For the SLC, DBH-ir neurons were commonly observed at (~AP = −9.50) through (~AP = −10.20) and spanned four to five sections per animal. Finally, for the C3, DBH-ir neurons were commonly observed from (~AP = −11.30) through (−AP = −12.60) and spanned six to eight sections per animal.

For each noradrenergic/adrenergic nucleus, the absolute number of DBH-ir neurons and the percentage of DBH-ir neurons that were retrogradely labeled from the MSA, MPOR, or SI was calculated for each animal and then averaged across all animals. This number represents the average percentage of retrogradely labeled DBH-ir neurons within a given nucleus. The total number of DBH-ir neurons and the total number of retrogradely labeled DBH-ir neurons across all noradrenergic/adrenergic nuclei were calculated in a subset of cases that received relatively large infusions that were well positioned within each basal forebrain region and that had consistent DBH staining throughout all nuclei. From these numbers, the percentage of all retrogradely labeled DBH-ir neurons (across all noradrenergic nuclei) was calculated for each animal and then subsequently averaged across animals. This number represents the relative distribution of all retrogradely labeled DBH-ir neurons across the individual nuclei.

In a subset of animals, analyses were conducted to examine the topography of FG retrogradely labeled neurons in the rostrocaudal and dorsoventral dimensions from both hemispheres in two to three adjacent series per animal. In the rostrocaudal analyses, the number of retrogradely labeled neurons was calculated from each of the three rostrocaudal levels (Figs. 1,6) and then summed across series for each animal. These values were subsequently averaged across animals and expressed as a percentage of the total number of retrogradely labeled neurons across the three levels of the LC to provide a value for each rostral, central, and caudal segment. For the dorsoventral analyses, each rostrocaudal extent of the LC was divided into three dorsoventral segments (Fig. 6). In these analyses, retrogradely labeled neurons were counted from each of the dorsoventral segments and then summed across series for each animal. These values were subsequently averaged across animals and expressed as a percentage of the total number of retrogradely labeled neurons across the three levels of the LC to provide a value for each dorsal, central, and ventral segment for each animal.

Brightfield photomicrographs were acquired by using an Axiocam HRc digital camera (Carl Zeiss, Thornwood, NY). Immunofluorescent photomicrographs were acquired by using a Nikon C1 confocal microscope (Nikon, Melville, NY). All digital images were matched for brightness and contrast by using Adobe (San Jose, CA) Photoshop 6.0 software and labeled by using Adobe Illustrator 10.0 software.

RESULTS

Boundaries of basal forebrain regions

To characterize better the organization of noradrenergic projections to basal forebrain arousal-related structures, FG or CTb was infused within the general regions of the MSA, MPOR, or SI. Previous studies delineated the boundaries for the MSA, MPOR, and SI within which noradrenergic α_1- and β-receptor agonists (MSA, MPOR) and/or hypocretin (SI) act to promote waking (Berridge and Foote, 1996; Berridge et al., 1996, 2003; Berridge and O'Neill, 2001; España et al., 2001; Thakkar et al., 2001). As defined by these previous sleep-wake studies, the MSA and MPOR are anatomically complex regions encompassing a number of distinct anatomical structures.

For example, the general region of the MSA contains neurons from the medial septum, the vertical limb of the diagonal band of Broca (NDB), the islands of Calleja, and relatively small portions of the lateral preoptic area (LPO; Swanson, 1998; Figs. 2, 3). The general region defined as the MPOR contains several preoptic structures, including the medial preoptic area proper (MPO), the medial preoptic nucleus (MPN), and the median preoptic nucleus (Swanson, 1998; Figs. 2, 3). Given the anatomical resolution of previously conducted microinfusion studies, the precise site(s) of action involved in the behavioral state modulatory actions of NE within the MSA and MPOR are not known. In contrast to the MSA and MPOR, the SI is a relatively homogenous region lacking multiple anatomically defined subnuclei (Swanson, 1998). Previous studies demonstrate that hypocretin acts to promote waking within the general region of the SI that includes the magnocellular preoptic area as well as the lateral and caudal portions of the NDB (España et al., 2001; Figs. 2, 3).

For the majority of cases, retrograde tracer infusions filled a substantial portion of a given basal forebrain region identified in these mapping studies as being sensitive to the sleep-wake modulatory actions of either NE or hypocretin.

General observations

MSA. FG infusions of sufficient size were made into the MSA in ten animals. In the majority of these cases, infusions largely targeted the medial septum and the vertical limb of the NDB (Figs. 2, 3). In four animals, FG infusions were located more ventrally, within the dorsalmost aspect of the horizontal limb of the NDB. In four of the above cases, a minute amount of infusate appeared to cross the midline.

Similar to that described previously (Vertes, 1988), infusion of a retrograde tracer within the MSA resulted in retrograde labeling widely throughout the rat brain. Within the forebrain, particularly dense labeling was observed within orbital (ORB) and infralimbic (ILA) areas of the cortex, the lateral septum, the vertical and horizontal limbs of the NDB, and the amygdala. Particularly high concentrations of labeled cells were also observed within

the anterior hypothalamic area and moderate levels within the medial preoptic area proper, the medial preoptic nucleus, and the ventrolateral preoptic area (VLPO). Throughout the thalamus, modest levels of retrograde labeling were observed.

Within the midbrain, relatively dense retrograde labeling was observed within the ventral tegmental area (VTA), the substantia nigra (SN), the periaqueductal gray (PAG), and the rostral aspects of the dorsal raphe. Within the pons and medulla, several regions showed moderate levels of retrograde labeling including the dorsal and lateral tegmental nuclei, the dorsal and median raphe nuclei, the raphe pallidus, and the LC (see below). Moderate levels of labeling were observed within the A1/C1 and A2/C2. Relatively few retrogradely labeled neurons were observed in other noradrenergic and adrenergic structures, such as the subcoeruleus (SLC), A7, A5, and A4. In all cases in which the FG infusion was largely unilateral, retrograde labeling was primarily observed ipsilateral to the infusion site (see below for further description). In contrast, when FG was infused bilaterally, retrograde labeling was also observed bilaterally.

MPOR. FG infusions were made into the MPOR in nine animals. In three of these animals infusions were confined to the ventromedial portion of the MPOR, encompassing the entire medial preoptic nucleus and the majority of the medial preoptic area proper, whereas in two cases infusions were placed more dorsally, immediately ventral to the anterior commissure (Figs. 2, 3). In three cases, the infusions encompassed the entire dorsoventral and mediolateral extent of the MPOR and the medial portions of the LPO. In one of these latter cases the infusions extended to the most caudal portions of the MPN. Additionally, in one animal the infusion was located lateral to the MPN and encompassed most of the medial preoptic area proper and a small portion of the LPO. Of the nine MPOR cases, four infusions resulted in tracer diffusion into the VLPO. In these cases, the magnitude and pattern of retrograde labeling obtained was similar to that observed in cases in which little or no tracer diffused into the VLPO.

Similar to that observed with FG infusions into the MSA and to that described previously, infusions of FG into the MPOR resulted in retrograde labeling widely throughout the brain (Vertes, 1988; Castañeyra-Perdomo et al., 1992). Dense retrograde labeling was observed within the lateral septum, the medial septum, and the bed nucleus of the stria terminalis (BNST). Lower concentrations of labeled cells were observed within the horizontal and vertical limbs of the diagonal band of Broca. Moderate levels of retrograde labeling were also observed throughout the thalamus and the amygdala.

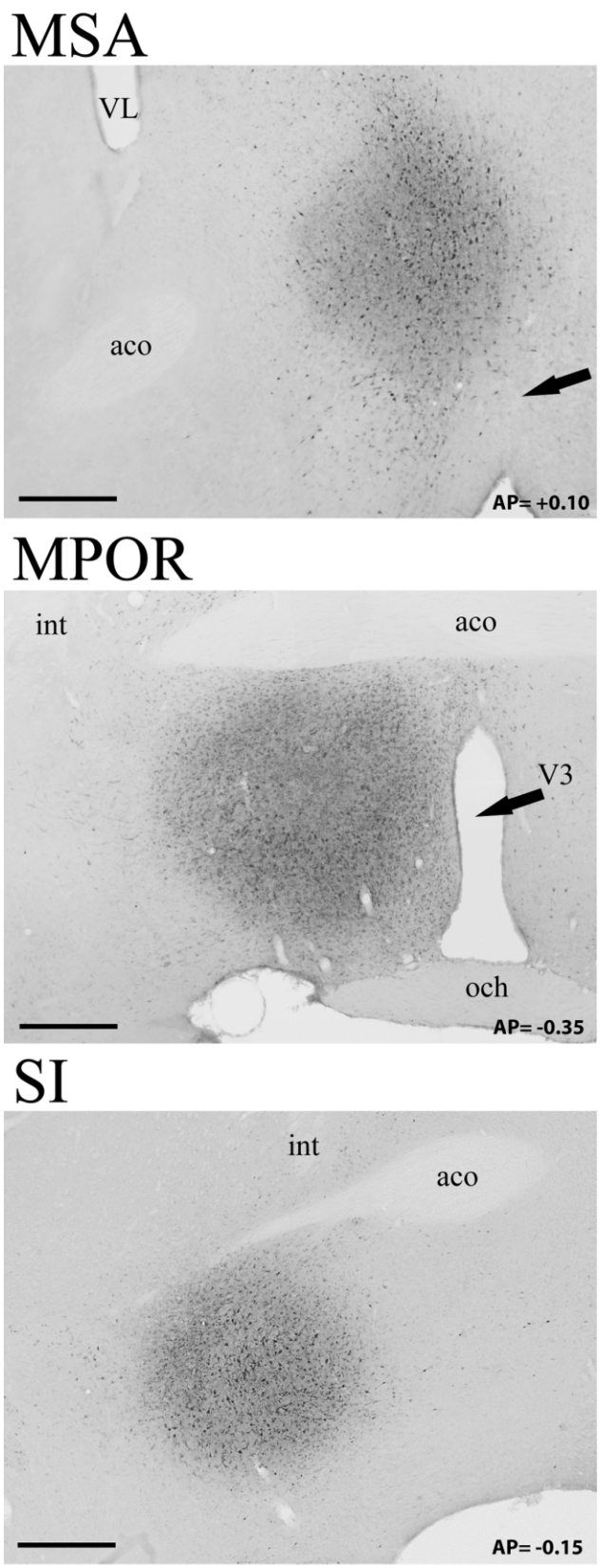

Fig. 2. Photomicrographs depicting representative FG infusions within MSA, MPOR, and SI. For MSA, the FG infusion is located largely within the medial septum and the dorsalmost aspects of the vertical limb of the diagonal band of Broca. For MPOR, the FG infusion is located within the medial and ventral aspects of MPOR. For SI, the FG infusion is located within the SI, immediately ventral to the anterior commissure and dorsal to the magnocellular preoptic area. For all regions, note the relatively well-demarcated border of the infusion with little diffusion into adjacent regions. The arrow points to midline. For abbreviations, see list. Scale bar = 500 μm.

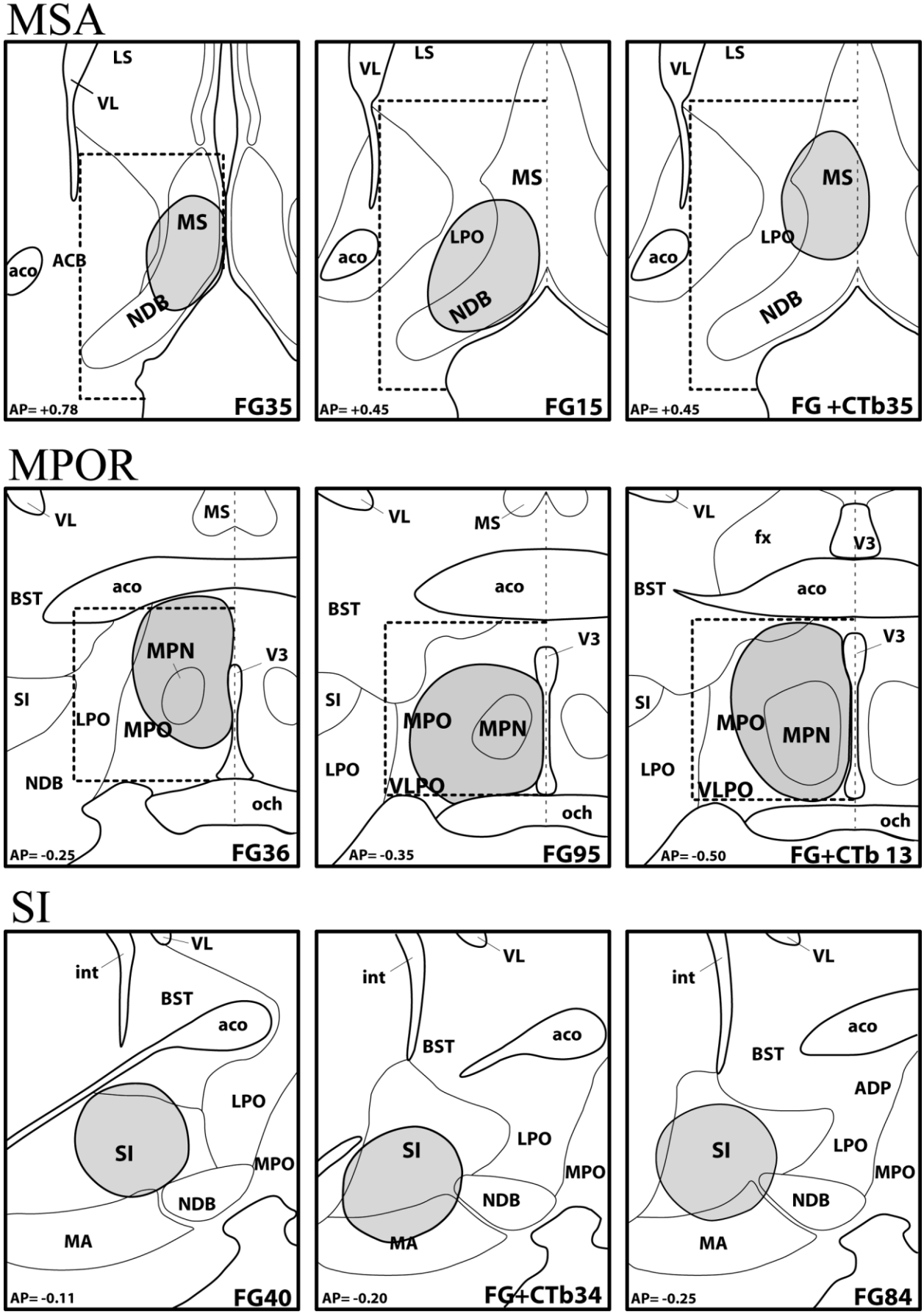

Fig. 3. Schematic depiction of approximate location of FG infusions within the MSA, MPOR, and SI. Shown are representative infusion locations within each region within a subset of three rats. The dotted lines denote the general area demonstrated previously as responsive to the wake-promoting actions of NE. AP numbers refer to approximate coronal level relative to bregma. For abbreviations, see list. Adapted from Swanson (1998).

In the midbrain, low-to-moderate levels of labeling were observed within the VTA, SN, and PAG. Within the pons and medulla, several regions showed low to moderate levels of retrograde labeling including the LC (see below), A1/C1, A2/C2, dorsal tegmental nucleus, laterodorsal tegmental nucleus, dorsal raphe, parabrachial nucleus, raphe magnus, and raphe pallidus. Few retrogradely labeled neurons were observed in the SLC, A4, A5, A7, and C3. In all cases, retrograde labeling was primarily observed ipsilateral to the infusion site.

SI. FG infusions were made into the general region of the SI in ten animals. In seven of these cases, infusions were largely confined to the SI (rostral Ch4; Mesulam et al., 1983) directly ventral to the anterior commissure and slightly rostral to the level of the decussation of the anterior commissure (Figs. 2, 3). In three additional animals, FG infusions were located more ventrally and encompassed the ventral aspects of the SI, portions of the posterior horizontal limb of the NDB, and the magnocellular preoptic nucleus.

Similar to that previously described, FG infusions into the SI resulted in retrograde labeling widely throughout the brain (Vertes, 1988; Grove, 1988; Semba et al., 1988; Jones and Cuello, 1989). Relatively dense labeling was observed within the ORB and ILA as well as throughout the anterior nucleus accumbens. More caudally, very dense labeling was observed within the nucleus accumbens, and lower levels of retrograde labeling were observed in the lateral septum, medial septum, NDB, and BNST. Relatively dense retrograde labeling was also observed within the VLPO, particularly in cases in which the FG infusion targeted ventral portions of the SI and dorsal portions of the magnocellular preoptic area. Modest levels of retrograde labeling were observed throughout the anterior and posterior hypothalamus, including the medial preoptic area proper. Moderate levels of retrograde labeling were also observed throughout the amygdala and the paraventricular nucleus of the thalamus.

In the midbrain, moderately dense labeling was observed within the VTA and PAG as well as low levels within the SN. Within the pons and medulla, several regions showed low to moderate levels of retrograde labeling including the dorsal tegmental nucleus, the laterodorsal tegmental nucleus, Barrington's nucleus, the LC (see below), the A1/C1, the A2/C2, the dorsal and central raphe, the parabrachial nucleus, the raphe linearis, and the raphe pallidus. Few retrogradely labeled neurons were observed in the SLC, A4, A5, A7, and C3. In all cases, retrograde labeling was observed primarily ipsilateral to the infusion site.

Origin of noradrenergic efferents to the MSA, MPOR, and SI

To characterize better the major sources of noradrenergic input to these basal forebrain regions, double-labeling immunohistochemistry was conducted and the distribution of DBH-ir neurons retrogradely labeled from FG or CTb infusions placed within the MSA (n = 7), MPOR, (n = 6), and SI (n = 8) was examined. In general, DBH-ir neurons were observed throughout the brainstem, as described previously (Lindvall and Bjorklund, 1983; Tucker et al., 1987; Saper et al., 1983). Briefly, in the rostrocaudal dimension, DBH-ir neurons were first observed within the A7 region at the level of the most rostral portions of Barrington's nucleus and the caudal extent of the dorsal raphe. These neurons were located lateral to the pontine reticular nucleus and ventral to the parabrachial nucleus and extended caudally for approximately 400 μm. LC DBH-ir neurons were first encountered in low numbers as a dispersed grouping of neurons in the same rostrocaudal plane as the posterior extent of the A7. More caudally, these neurons formed a small round nucleus, which subsequently became increasingly larger and more compact, forming the main body of the LC (Fig. 1). LC DBH-ir neurons eventually transitioned into A4 neurons, which lined the dorsolateral fourth ventricular wall and extended approximately 1 mm beyond the LC. DBH-ir neurons within the SLC emerged immediately ventral to the central main body portions of the LC (Fig. 1, Central) as a small grouping of neurons that persisted for approximately 300 μm. At levels that contained the caudalmost portions of the LC, SLC neurons were no longer present. A5 DBH-ir neurons were generally encountered in alignment with the caudal third of the LC. This small collection of neurons was located dorsal to the lateral superior olivary nucleus and extended approximately 700 μm beyond the LC immediately caudal to the VII nerve.

The adrenergic C3 region began approximately 500 μm caudal to the A5 and 100 μm caudal to the A4. These neurons were principally located medial and ventral to the nucleus propositus and paragigantocellular reticular nucleus and extended caudally for nearly 1 mm. Within this range, DBH-ir neurons within the adrenergic C1 region were encountered at the level of the nucleus raphe obscurus, immediately ventral to the VII nerve. These adrenergic neurons (Saper et al., 1983) extended caudally where they briefly intermixed with noradrenergic neurons and eventually gave way to form the A1 region within the ventrolateral border of the reticular formation, medial and ventral to the spinal trigeminal nucleus. A1 neurons continued for approximately 2 mm into the cervical 1 level of the spinal cord. Similar to the C1, DBH-ir neurons within the adrenergic C2 region were initially encountered at the level of the nucleus raphe obscurus, along the medial edge of the nucleus of the solitary tract (NTS). Caudally, this group of DBH-ir neurons migrated medially for approximately 500 μm where it divided into two loose clusters: 1) a dorsal collection of neurons forming an arc medial to the NTS and ventral to the fourth ventricle; and 2) a more ventral collection abutting the medial border of the dorsal motor nucleus of the vagus (Saper et al., 1983, 1993). At levels caudal to the more posterior aspects of the reticular nucleus, A2 DBH-ir neurons formed a single compact cluster within the ventromedial commissural NTS, dorsal to the central canal. This cluster extended caudally for approximately 2 mm.

Using standard immunoperoxidase/brightfield techniques, the extent of retrograde labeling of DBH neurons (DBH + FG) was examined across *all* noradrenergic/adrenergic nuclei in a subset of animals (n = 3 per region) in which: 1) FG infusions were centered within the basal forebrain region of interest; 2) FG was distributed uniformly throughout the majority of the region of interest, and; 3) consistent DBH staining was obtained throughout the rostral-caudal extent of all noradrenergic/adrenergic nuclei. To ensure the reliability and accuracy of immunoperoxidase analyses, in adjacent sections, retrogradely labeled DBH-ir neurons in the LC were also visualized by using immunofluorescent techniques (see Materials and Methods). Results obtained from these analyses demon-

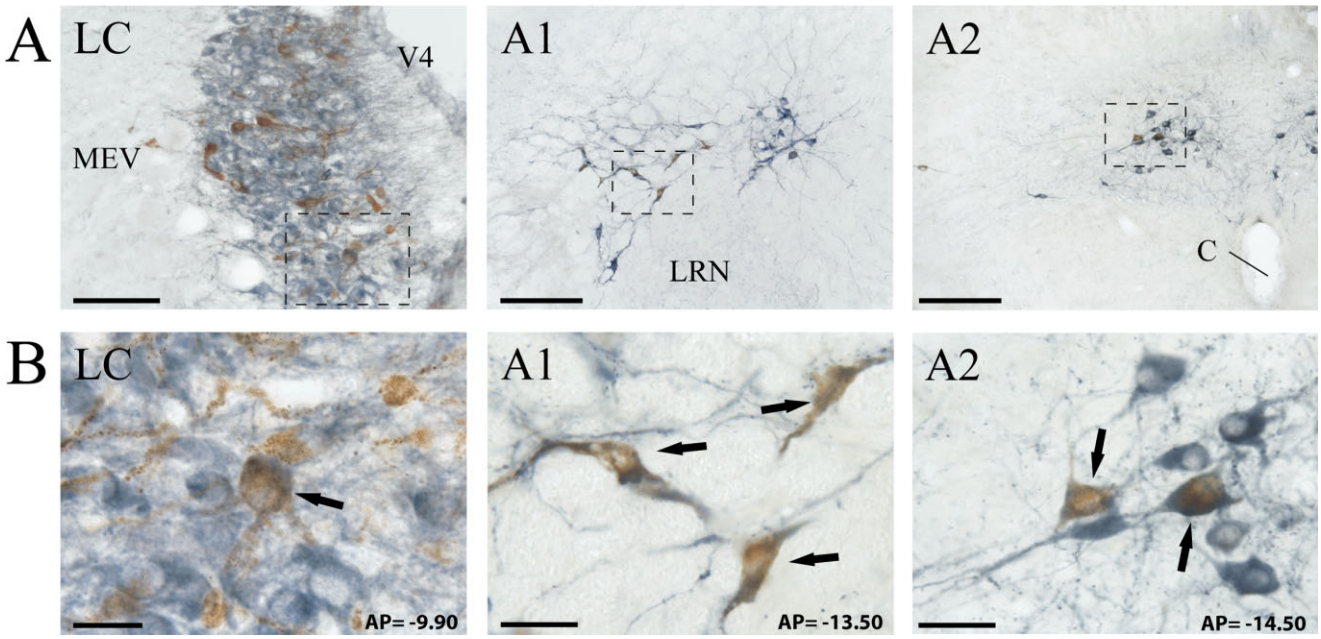

Fig. 4. Photomicrographs depicting retrogradely labeled DBH-ir neurons within select noradrenergic nuclei. Shown are low (**A**) and high (**B**) magnification images of FG-labeled neurons (brown), DBH-ir neurons (blue), and FG-labeled DBH-ir neurons (blue-brown) within the LC, A1, and A2 from one rat infused with FG into MSA. Boxes in A indicate regions displayed at higher magnification in B. Arrows indicate examples of retrogradely labeled DBH-ir neurons. Note that retrogradely labeled DBH-ir neurons are observed within the LC, A1, and A2. AP numbers refer to approximate coronal level relative to bregma. For abbreviations, see list. Scale bars = 100 μm in A; 25 μm in B.

strate comparable numbers of retrogradely labeled DBH-ir neurons using both immunoperoxidase and immunofluorescent techniques (Figs. 4, 5). For example, by using immunoperoxidase methods, the mean number of retrogradely labeled DBH-ir neurons in the LC (three rostrocaudal levels of LC) following FG infusions into the MSA, MPOR, and SI was 13.1 ± 0.8, 10.9 ± 1.2, and 11.4 ± 0.7, respectively. By using immunofluorescent methods, we obtained cell counts of 14.1 ± 1.3, 11.4 ± 1.7, and 11.9 ± 1.1, for the MSA, MPOR, and SI, respectively. Combined with previous observations comparing results obtained with both peroxidase and fluorescent techniques (España et al., 2005), these observations suggest accurate estimation of the number of double-labeled neurons using this immunoperoxidase-based brightfield protocol. Based on these results, all further analyses were conducted by using immunoperoxidase staining and brightfield microscopy.

MSA. Infusions of FG or CTb into the MSA resulted in retrograde labeling of DBH-ir neurons within noradrenergic nuclei located throughout the brainstem (Figs. 4, 5; Table 1). Across all DBH-ir neurons counted within all brainstem adrenergic nuclei, the majority of the double labeling was observed within the LC (56.8 ± 5.8%) and considerably less double labeling was observed within the A1/C1 (23.6 ± 4.9%) and A2/C2 (14.5 ± 1.7%). Minimal to no double labeling was observed within the A5, SLC, A7, or C3. Retrogradely labeled non-DBH neurons were frequently observed within the anterior aspect of the LC and the A1/C1 and A2/C2 regions. In two cases, FG infusions were placed within the shell subregion of the nucleus accumbens with minimal to no encroachment into the general region of the MSA. Consistent with that described previously (Delfs et al., 1998), in these two cases the majority of double labeling was observed within the A1/C1 (44.6 ± 1.9%), and lesser labeling was observed within the LC (27.6 ± 5.4%), A2/C2 (24.7 ± 5.3%), and A5 (2.4 ± 1.6%).

MPOR. Infusions of FG into the MPOR resulted in retrograde labeling of DBH-ir neurons within several noradrenergic nuclei (Table 1). Although the LC contained a large number of double-labeled neurons (41.7 ± 2.2%), a similar number of double-labeled neurons were also observed within the A1/C1 region of the medulla (39.7 ± 1.8%). Considerably less double labeling was observed within the A2/C2 (14.9 ± 1.8%) and A5 (2.9 ± 0.6%). Little to no double labeling was observed within the A4, A7, and C3. As with MSA tracer infusions, retrogradely labeled non-DBH neurons were frequently observed within the anterior aspect of the LC and the A1/C1 and A2/C2 regions.

SI. In a subset of animals described above, infusions of FG into the SI resulted in retrograde labeling of DBH-ir neurons within several noradrenergic nuclei (Table 1). The majority of the double labeling was observed within the LC (46.8 ± 2.5%), and less labeling was observed within the A1/C1 (24.8 ± 2.9%), A2/C2 (21.1 ± 3.3%), and A5 (6.0 ± 2.4%). Minimal to no double labeling was observed within the A4, A7, and C3. As with the MSA and MPOR tracer infusions, retrogradely labeled non-DBH neurons were frequently observed within the anterior aspect of the LC and the A1/C1 and A2/C2 regions.

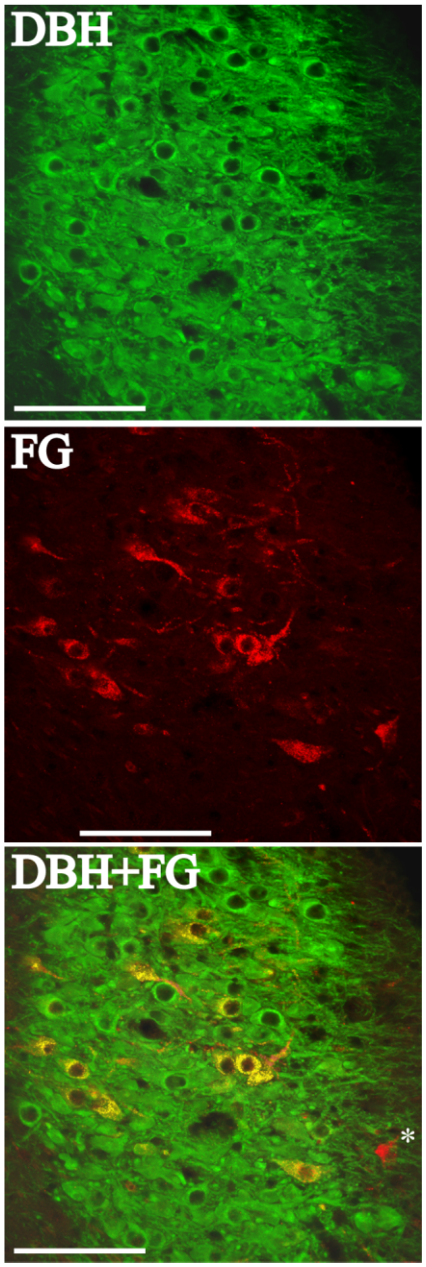

Fig. 5. Fluorescent photomicrographs depicting retrogradely labeled DBH-ir neurons within the LC from one rat infused with FG in the MSA. Shown are DBH-ir neurons (green, top panel), FG-retrogradely labeled neurons (red, center panel), and FG-retrogradely labeled DBH-ir neurons (yellow, bottom panel) derived from a composite of DBH and FG photomicrographs. Asterisk indicates an example of a retrogradely labeled neuron that is not DBH-ir. For Abbreviations, see list. Scale bar = 100 μm.

TABLE 1. Distribution of Retrogradely Labeled DBH-ir Neurons Across Select Noradrenergic Nuclei Following Tracer Infusion Into the Basal Forebrain[1]

Region	No. of DBH-ir neurons per region	% DBH-ir neurons retrogradely labeled per region	% of all DBH-ir neurons retrogradely labeled
MSA			
LC (A6)	52.3 ± 7.4	23.6 ± 2.7	56.8 ± 5.8
SubC	7.7 ± 10.8	1.1 ± 0.7	0.5 ± 0.3
A1/C1	12.7 ± 0.8	14.3 ± 2.4	23.6 ± 4.9
A2/C2	14.5 ± 1.7	9.6 ± 5.3	16.0 ± 2.5
A4	3.9 ± 0.5	0.0 ± 0.0	0.0 ± 0.0
A5	6.2 ± 0.7	4.9 ± 1.3	1.8 ± 1.0
A7	9.5 ± 1.7	1.1 ± 1.1	0.3 ± 0.3
C3	5.3 ± 0.7	1.5 ± 1.5	1.0 ± 1.0
MPOR			
LC (A6)	56.4 ± 8.0	15.5 ± 2.0	41.7 ± 2.2
SubC	6.7 ± 0.8	0.0 ± 0.0	0 ± 0.0
A1/C1	10.9 ± 0.7	25.8 ± 2.9	39.5 ± 1.8
A2/C2	16.9 ± 2.1	5.8 ± 1.1	14.9 ± 1.8
A4	2.6 ± 0.3	0.0 ± 0.0	0.0 ± 0.0
A5	6.4 ± 0.7	8.3 ± 2.8	2.9 ± 0.6
A7	6.6 ± 1.7	2.0 ± 2.0	0.3 ± 0.3
C3	4.0 ± 0.5	6.2 ± 4.5	0.7 ± 0.4
SI			
LC (A6)	57.5 ± 9.0	16.1 ± 2.4	46.8 ± 2.5
SubC	7.5 ± 1.2	0.0 ± 0.0	0 ± 0.0
A1/C1	11.5 ± 0.9	12.9 ± 2.1	24.8 ± 2.9
A2/C2	15.3 ± 2.0	9.58 ± 1.7	21.1 ± 3.3
A4	5.5 ± 0.8	6.7 ± 2.9	1.0 ± 0.1
A5	9.2 ± 0.7	5.4 ± 1.2	6.0 ± 2.4
A7	6.8 ± 2.6	1.4 ± 1.4	0.4 ± 0.4
C3	4.5 ± 0.5	0.0 ± 0.0	0 ± 0.0

[1]Shown are: 1) mean number (± SEM) of DBH-ir neurons per noradrenergic/adrenergic nucleus; 2) percentage (± SEM) of DBH-ir neurons from each noradrenergic nucleus that were retrogradely labeled from the respective basal forebrain region (MSA, MPOR, or SI); and 3) percentage of the total number of DBH-ir neurons across all noradrenergic nuclei that were retrogradely labeled within a given noradrenergic nucleus. For each basal forebrain region the majority of DBH-ir retrogradely labeled neurons was observed within the LC and a lesser percentage within A1/C1 and A2/C2. Values shown were obtained by applying Abercrombie's correction factor (Abercrombie and Johnson, 1946). For abbreviations, see list.

TABLE 2. Topographical Distribution of Retrograde Labeling Within the LC Following Retrograde Tracer Infusion Into the MSA, MPOR, and SI[1]

Region	Rostral (%)	Central (%)	Caudal (%)
Rostrocaudal			
MSA	38.4 ± 4.8	41.6 ± 3.3	20.0 ± 3.0
MPOR	42.7 ± 5.6	29.3 ± 5.7	28.0 ± 6.4
SI	42.2 ± 4.0	33.4 ± 2.7	24.3 ± 3.0
Region	Dorsal	Central	Ventral
Dorsoventral			
MSA	45.4 ± 4.9	33.3 ± 3.4	21.2 ± 3.1
MPOR	30.7 ± 6.3	43.5 ± 4.2	25.8 ± 4.2
SI	40.2 ± 3.4	39.2 ± 2.1	20.6 ± 2.4

[1]Shown are the percentages of FG retrogradely labeled neurons located across the rostrocaudal and dorsoventral extents of the LC following tracer infusion into the MSA, MPOR, or SI. For each basal forebrain region the majority of resulting retrograde labeling was observed, rostrocaudally, within the rostral and central portions of LC. Dorsoventrally, the majority of retrograde labeling was observed within the dorsal and central thirds of the LC. Values shown are derived from cell counts adjusted by using Abercrombie's correction (Abercrombie's and Johnson, 1946). Values shown were obtained by applying Abercrombie's correction factor (Abercrombie and Johnson, 1946). For abbreviations, see list.

Organization of LC efferents to the MSA, MPOR, and SI

To examine the extent to which LC neurons projecting to forebrain arousal-related structures are lateralized and topographically organized, the retrograde tracer FG was infused within the MSA, MPOR, or SI, and retrograde labeling was examined within the LC. In all cases examined, infusions of FG within these basal forebrain structures resulted in retrograde labeling within the LC (Tables 1, 2).

For the MSA, retrogradely labeled cells were observed primarily ipsilaterally within the LC (83.9 ± 1.9% ipsilateral vs. 16.1 ± 1.9% contralateral). Results obtained from topographical analyses conducted on a subset of animals (n = 6) indicated that, rostrocaudally, retrograde labeling was concentrated to the rostral (38.4 ± 4.8%) and central

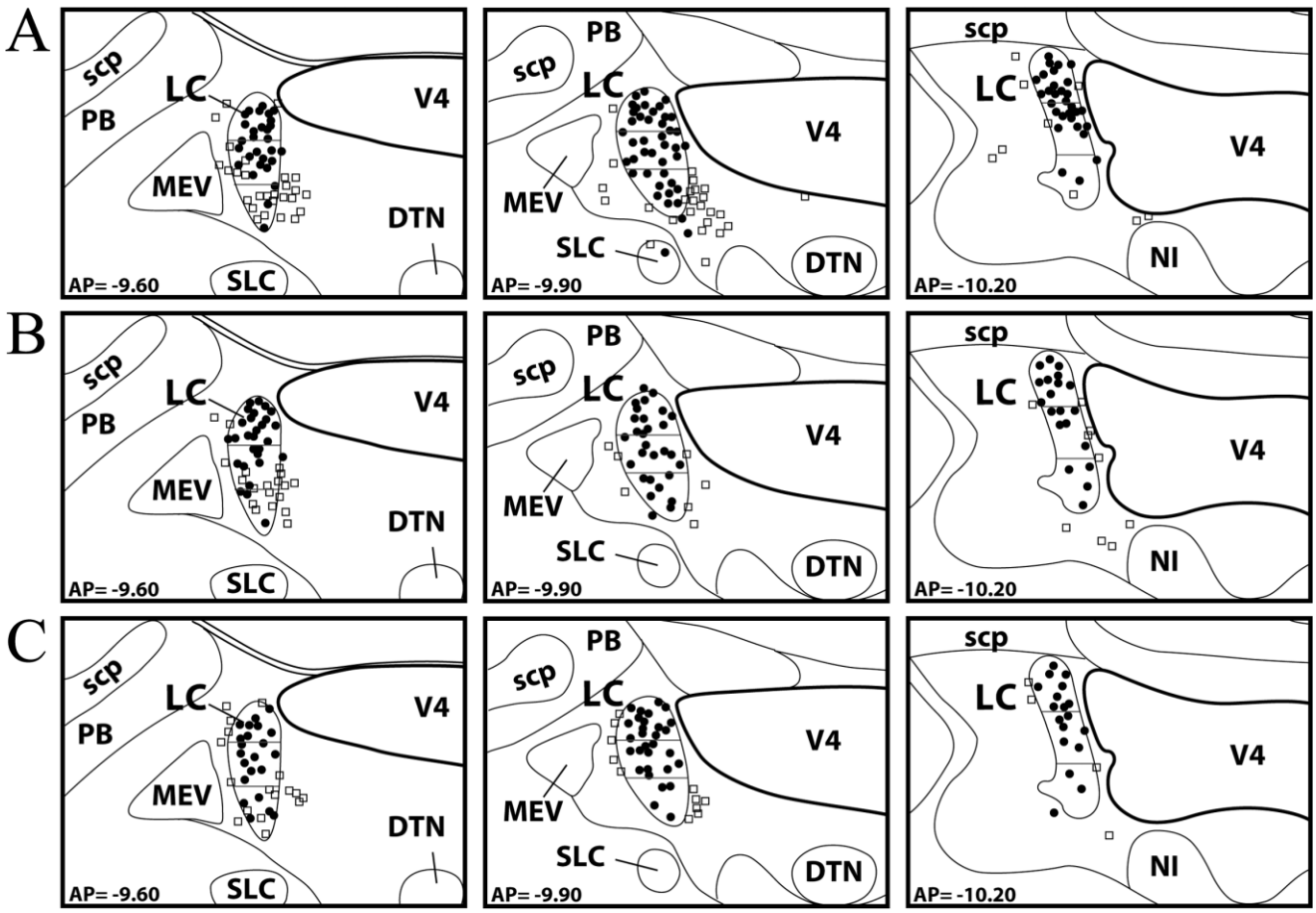

Fig. 6. Schematic depiction of the topographical distribution of retrogradely labeled neurons within LC. Shown are three representative rostrocaudal levels of the LC in three separate rats that received injection of FG into either the (**A**) MSA, (**B**) MPOR, or (**C**) SI. Within each rostrocaudal level, the LC was divided into three dorsoventral segments for topographical analyses (see Materials and Methods). Filled circles represent one DBH-ir neuron retrogradely labeled from the respective basal forebrain structure. Open squares represent a non-DBH-ir neuron retrogradely labeled. In all cases, the majority of retrogradely labeled DBH-ir neurons are located within the rostral and central portions of the LC, in the rostrocaudal dimension. In the dorsoventral dimension, the majority of retrogradely labeled DBH-ir neurons are observed within the dorsal and central thirds of the LC. AP numbers refer to approximate coronal level relative to bregma. For abbreviations, see list. Adapted from Swanson (1998).

portions (main body; 41.6 ± 3.3%) of the LC, although labeling was also observed within the caudal third of the LC (20.0 ± 3.0%). Dorsoventrally, the most consistent and densest labeling was observed within the dorsal (45.4 ± 4.9%) and central thirds (33.3 ± 3.4%) of the LC, although labeling was observed within the ventral third as well (21.2 ± 3.1%; Fig. 6A).

Similar to that observed with the MSA, FG infusions placed within the MPOR (n = 6) resulted in retrograde labeling throughout the LC nucleus. In all cases examined, retrogradely labeled cells were observed primarily ipsilateral (81.4 ± 6.6% ipsilateral vs. 18.6 ± 3.1% contralateral) to the infusion site. Rostrocaudally, a slight majority of retrogradely labeled neurons was observed within the rostral third of the LC (42.7 ± 5.6%). The remaining retrograde labeling was distributed equally between the central (29.3 ± 5.7%) and caudal (28.0 ± 6.4%) portions of the LC. Dorsoventrally, the highest levels of retrograde labeling were observed within the central (43.5 ± 4.2%) third of the LC, although labeling was also consistently observed within the dorsal (30.7 ± 6.3%) and ventral (25.8 ± 4.2%) thirds (Fig. 6B).

Similar to that observed with infusions into the MSA and MPOR, FG infusions placed within the SI (n = 6) resulted in retrograde labeling throughout the LC nucleus. In all cases examined, retrogradely labeled cells were observed primarily ipsilaterally (81.7 ± 2.4% ipsilateral vs. 18.3 ± 2.4% contralateral) within the LC. Rostrocaudally, retrogradely labeled neurons were distributed throughout the LC with the majority of labeled cells located within the rostral (42.2 ± 4.0%) and central (33.4 ± 2.7%) portions of the LC and lesser labeling observed within the caudal portion of the LC (24.3 ± 3.0%). Dorsoventrally, retrograde labeling was primarily observed within the dorsal (40.2 ± 3.4%) and central (39.2 ± 2.1%) thirds, although labeling was also consistently observed within the ventral (20.6 ± 2. 4%) third (Fig. 6C).

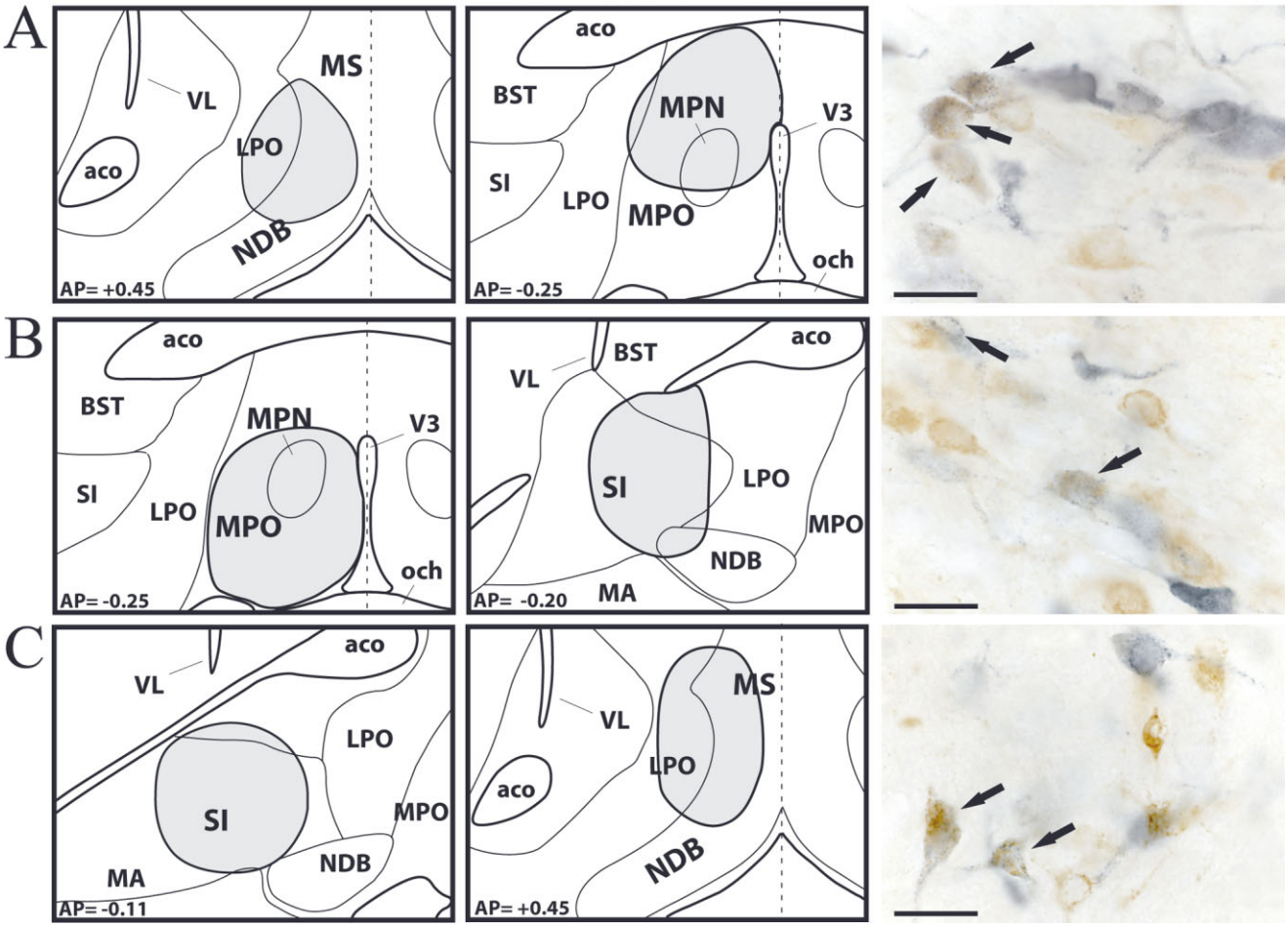

Fig. 7. Schematic depiction of approximate locations of dual retrograde tracer infusions within two basal forebrain sites and photomicrographs of the resulting retrograde labeling within the LC. Shown are FG and CTb infusion locations within (**A**) the MSA and MPOR; (**B**) the MPOR and SI; and (**C**) the SI and MSA. The resulting retrograde labeling associated with each of these combinations of infusions is also shown. CTb (brown), FG (blue), and FG+CTb (blue-brown) labeled neurons are shown within the central portion of the LC. Arrows point to neurons retrogradely labeled with FG and CTb from injections made into the two respective basal forebrain regions (e.g., the MSA and MPOR in A). AP numbers refer to approximate coronal level relative to bregma. For abbreviations, see list. Adapted from Swanson (1998). Scale bar = μm in A–B

Dual retrograde labeling of LC neurons following infusions of retrograde tracer into two distinct basal forebrain regions

To examine whether projections of individual LC neurons collateralize to two distinct basal forebrain structures, 12 rats were injected with both FG and CTb within two of the three basal forebrain regions described above (e.g., the MSA + MPOR; MSA + SI; MPOR + SI). For any given pair of regions, tracer infusions were counterbalanced such that each region received each tracer. The following groups of animals were examined; 1a) FG in the MSA + CTb in the MPOR (n = 2); 1b) CTb in the MSA + FG in the MPOR (n = 2); 2a) FG in the MSA + CTb in the SI (n = 2); 2b) CTb in the MSA + FG in the SI (n = 2); 3a) FG in the MPOR + CTb in the SI (n = 2); and 3b) CTb in the MPOR + FG in the SI (n = 2). Examples of infusions of FG and CTb within these basal forebrain regions are shown in Figures 3 and 7.

In general, within all regions examined, CTb infusions resulted in levels of retrograde labeling comparable to those observed with FG infusions. In some cases, however, slightly higher levels of retrograde labeling were observed within the ipsilateral and contralateral hemispheres following CTb infusions. This difference in levels of retrograde labeling might be due, in part, to the infusion procedures used for each retrograde tracer (e.g., pressure vs. iontophoresis; see Discussion).

Double-labeling immunohistochemistry was conducted to examine collateralization of LC efferents to two distinct basal forebrain regions. These studies indicated that in cases in which infusions were placed within both the MSA and MPOR, 33.9 ± 6.5% of LC neurons retrogradely labeled from the MSA were also retrogradely labeled from the MPOR. Conversely, 26.0 ± 7.8% of LC neurons retrogradely labeled from the MPOR were also retrogradely labeled from the MSA (Fig. 7a). In cases in which infu-

sions were placed within the MPOR and SI, 26.7 ± 6.2% of LC neurons retrogradely labeled from the MPOR were also retrogradely labeled from the SI. Conversely, 22.6 ± 3.5% of LC neurons retrogradely labeled from the SI were also retrogradely labeled from the MPOR (Fig. 7B). Finally, in cases in which infusions were placed within the SI and MSA, 38.1 ± 7.5% of LC neurons retrogradely labeled from the SI were also retrogradely labeled from the MS (Fig. 7C). Conversely, 39.0 ± 8.0% of LC neurons retrogradely labeled from the MSA were also retrogradely labeled from SI.

Consistent with observations from retrograde tracing studies in individual basal forebrain regions, the majority of LC neurons double-labeled from two basal forebrain regions were located rostrocaudally within the rostral and central portions of the LC and, dorsoventrally, within the dorsal and central thirds of the LC (data not shown). For all cases examined, relatively low levels of double labeling were observed within the contralateral hemisphere.

DISCUSSION

Noradrenergic efferents act within a circumscribed region of the medial basal forebrain to promote waking (e.g., the MSA and MPOR). Interestingly, although the SI plays a critical role in the regulation of cortical EEG and behavioral activity state (Buzsaki et al., 1988; Metherate et al., 1992; España et al., 2001; Thakkar et al., 2001) and NE modulates SI neuronal activity (Fort et al., 1995), this region is relatively insensitive to the wake-promoting actions of NE and noradrenergic agonists (Berridge and Foote, 1996; Berridge et al., 1996, 2003; Berridge and O'Neill, 1999). The basic features of the LC-noradrenergic innervation of these basal forebrain arousal-related structures have been described previously (Segal and Landis, 1974; Jones and Moore, 1977; Moore, 1978; Krayniak et al., 1981; Valentino et al., 1983; Zaborsky, 1989). Nevertheless, much remained unknown concerning the sources of noradrenergic input to these regions, the topographic organization of basal forebrain-projecting LC neurons, and the extent to which individual LC neurons simultaneously target these arousal-related regions.

Organization of LC efferents to the basal forebrain

These studies demonstrate that despite differences in sensitivity to the wake-promoting actions of NE across these basal forebrain regions, the origin and organization of noradrenergic efferents is largely similar for these three regions. In each case, the LC is a major source of noradrenergic input to these three regions. Thus, across all DBH-ir neurons retrogradely labeled in these studies, approximately 50% were located within the LC. Nonetheless, both the A1/C1 and A2/C2 provide substantial noradrenergic/adrenergic input to the MSA, MPOR, and SI. In the case of the MPOR, input from the A1/C1 (39.5%) was largely comparable to that of the LC (41.7%), consistent with previous observations that the A1 and C1 both project to the median preoptic nucleus (Armstrong et al., 1983; Saper et al., 1983; Tucker et al., 1987). In contrast, the A1/C1 provides substantially less input to the MSA (23.6%) and SI (24.8%).

In the current study, we did not differentiate noradrenergic vs. adrenergic cell bodies (e.g., the A1 vs. C1, the A2 vs. C2). However, when these structures were differentiated on the basis of anatomical landmarks (Tucker et al., 1987; Paxinos et al., 1999), substantial labeling was observed within the presumed adrenergic nuclei C1 and C2. Thus, following FG infusion into the MPOR, 22.2 ± 2.0 % of all double-labeled neurons were located within the C1. Consequently, only 17.3 ± 1.2 % of neurons estimated to be located within the A1 were double-labeled. This is consistent with previous observations indicating that approximately 50% of ventrolateral medullary neurons retrogradely labeled from tracer infusion into the median preoptic nucleus were adrenergic and not noradrenergic (Saper et al., 1983). Therefore, the above-described analyses probably overestimate the *noradrenergic* contribution to these basal forebrain regions arising from the ventrolateral medullary nuclei. In contrast, the C2/A2 region appears to provide minimal adrenergic innervation to the median preoptic nucleus (Saper et al., 1983). For all basal forebrain regions examined, substantially less noradrenergic input arises from the region of the A5 (1.5–6%) and lesser input still from the SLC, A4, and A7.

The pattern of sources of noradrenergic input to these basal forebrain regions differs from that observed with the nucleus accumbens shell and VLPO, both of which lie within close proximity to the MSA and MPOR/SI, respectively, and which receive sparse input from the LC (see Results; Delfs et al., 1998; Chou et al., 2002). Combined, these observations indicate that different subfields of the basal forebrain have highly divergent sources of noradrenergic input. This provides the anatomical substrate for the differential regulation of noradrenergic neurotransmission across adjacent basal forebrain structures. The functional significance of this segregation of noradrenergic input remains to be determined. However, it is worth noting that the LC receives prominent input from forebrain regions associated with higher cognitive and affective function (e.g., prefrontal cortex, amygdala; Arnsten and Goldman-Rakic, 1984; Van Bockstaele et al., 1998; for review see Berridge and Waterhouse, 2003). Thus, basal forebrain regions receiving substantial LC input are likely to be influenced by these cortical and subcortical forebrain regions involved in cognition and affect.

The majority of LC noradrenergic efferents to each of these basal forebrain regions originated from the ipsilateral hemisphere (approx. 80–85%). The proportion arising from the contralateral hemisphere is substantially larger than that observed for the neocortex but less than that observed for certain thalamic and brainstem sensory structures (Simpson et al., 1997). Therefore, in terms of lateralization, the LC innervation of these basal forebrain arousal-related regions appears to be somewhat intermediate between cortical and certain other subcortical structures. When discussing laterality of noradrenergic efferents to these basal forebrain regions, it is important to note that stimulation of NE receptors unilaterally within the MSA and MPOR results in the bilateral activation of forebrain EEG and alert waking (Berridge and Foote, 1996; Berridge et al., 1996; Berridge and O'Neill, 2001). It is not known whether the 15–20% of LC fibers that innervate the contralateral MSA and MPOR are sufficient to drive alterations in EEG and behavioral activity states. However, as far as is known, LC neurons respond similarly across the two hemispheres to environmental stimuli. Given this, under normal conditions, alterations in rates of NE release will occur simultaneously within both

hemispheres of the basal forebrain, ensuring coordination of noradrenergic neurotransmission within each hemisphere.

Within the LC, there was a slight bias for basal forebrain-projecting neurons to be located, rostrocaudally, within the rostral and central portions of the LC and, dorsoventrally, within the dorsal and central portions of the LC. Nonetheless, in general, basal forebrain-projecting neurons were observed throughout the rostrocaudal and dorsoventral extent of the LC. This is in contrast to that described previously for LC neurons projecting to the neocortex, hippocampus, cerebellum, and spinal cord (Loughlin et al., 1986), which tend to display distinct topographic distributions within the nucleus. Thus, basal forebrain-projecting LC neurons appear to be more uniformly distributed within the LC than LC neurons projecting to these other regions. A similarly broad distribution of retrograde tracer within the LC was observed following infusions into the ventromedial nucleus of the hypothalamus (Loughlin et al., 1986). Additionally, the broad distribution of basal forebrain-projecting LC neurons across the dorsoventral dimension is similar to that described for the frontal cortex (Waterhouse et al., 1983).

LC neurons projecting to these basal forebrain regions did not appear to be segregated within the LC. Consistent with this, we observed a high degree of collateralization of individual LC neurons across the three basal forebrain regions. This indicates a substantial proportion of individual LC neurons that project to one of these basal forebrain regions simultaneously projects to the other two regions. The highest degree of collateralization was observed for tracer infusions into the MSA and SI (e.g., approximately 40%), whereas the lowest degree of collateralization was observed between the MPOR and SI (e.g., approximately 25%). As discussed below, tracer infusions did not completely fill a given region, and thus these analyses probably underestimate the degree of collateralization of LC neurons across these basal forebrain regions.

Methodological considerations

Infusion volume is a critical variable in the use of retrograde tracers (Ader et al., 1980). In the current study, infusion volumes were used that resulted in diffusion of tracer throughout a substantial portion of the targeted region, while avoiding diffusion into adjacent structures. The use of infusions of FG or CTb that did not fill entirely a given structure probably results in an underestimation of the absolute number of LC neurons that project to a given structure. None of the retrograde tracer infusions filled more than one-half of any given region, and most filled substantially less than this. Therefore, it is estimated that at least two to four times higher levels of retrograde labeling of LC neurons and higher levels of collateralization across basal forebrain regions would have been observed had an entire field been filled with retrograde tracer.

Previous mapping studies indicate wake-promoting actions of NE and other neurotransmitters within the general regions MSA, MPOR, and SI (Kumar et al., 1986; Mallick and Alam, 1992; Berridge and Foote, 1996; Berridge et al., 1996, 1999, 2003; Berridge and O'Neill, 2001; España et al., 2001; Thakkar et al., 2001). As defined in these studies, these regions are relatively large and anatomically complex. Thus, the region defined as the MSA and identified as being sensitive to the wake-promoting actions of NE and hypocretin encompasses the medial septum, the vertical limb of the diagonal band of Broca, the islands of Calleja, and relatively small portions of the LPO (Swanson, 1998). In the case of the MPOR, NE and hypocretin promote waking within a region encompassing the medial preoptic area proper, the medial, median, anterodorsal, and anteroventral preoptic nuclei, and the anteroventral periventricular nucleus of the hypothalamus (Swanson, 1998). The current experiments were aimed at a better understanding of the anatomical organization underlying the wake-promoting actions of NE within these general basal forebrain regions. As such, these studies utilized moderately large infusions that resulted in the distribution of retrograde tracer throughout a substantial portion of a given region previously identified as being sensitive to the wake-promoting actions of NE. It remains for future studies, using more restricted tracer infusions, to characterize NE efferents to individual subnuclei contained within these general regions.

For FG infusions into the MSA, in some cases infusate may have encroached on the medial portion of the nucleus accumbens. However, in two cases in which an FG infusion was made directly into the nucleus accumbens shell while avoiding more medial structures including the medial septum and NDB, low levels of retrograde labeling were observed within the LC and higher levels within the regions of the A1 and A2. This pattern is quite distinct from that observed following tracer infusion into the MSA. Thus, it does not appear that uptake of retrograde tracer from either shell or core subregions of the nucleus accumbens contributed substantially to the labeling of hypocretin neurons observed following infusions into the MSA. In the case of the MPOR, all infusions were concentrated within the medial portions of this general region with little or no diffusion into the bed nucleus of the stria terminalis or LPO. Comparable patterns and density of labeling were observed following infusions into medial, lateral, dorsal, and ventral portions of the general region of the MPOR. Infusions that targeted the SI were well contained within the borders of this region and did not result in diffusion outside of the SI region. Nevertheless, in two cases, infusions of FG were made within the ventral portion of the SI that resulted in substantial diffusion of FG into the posterior horizontal limb of the the NDB and the magnocellular preoptic nucleus. In these two cases, however, retrograde labeling within the LC appeared to be indistinguishable from that observed with infusions placed more dorsally within the SI.

It is generally accepted that FG and CTb, as well as other retrograde tracers, can be taken up by fibers of passage, although this appears to be minimal with iontophoretic application compared with pressure injection (Pieribone and Aston-Jones, 1988). The slightly higher levels of retrograde labeling observed in the current studies with CTb pressure ejection versus FG iontophoretic ejection may, in part, reflect variations in the degree to which these tracers were taken up by fibers of passage. However, the fact that both qualitatively and quantitatively similar patterns of retrograde labeling were observed with iontophoretic and pressure ejection of tracers suggests that results obtained in the present study accurately reflect the pattern of LC efferents to these basal forebrain regions.

Functional implications

The regulation of both forebrain neuronal activity state and behavioral state involves a large array of brainstem and forebrain systems. Included within these systems are noradrenergic efferents innervating the MSA, MPOR, and SI. The current studies suggest that the LC is the primary source of noradrenergic innervation of these basal forebrain regions, although the dorsal and ventrolateral medullary adrenergic/noradrenergic nuclei (A1/C1, A2/C2) provide a moderate-to-substantial contribution to this innervation (particularly in the case of the MPOR). The LC plays a critical role in a wide array of perceptual, cognitive, and affective processes (for review, see Berridge and Waterhouse, 2003). These diverse actions of the LC-noradrenergic system involve actions of NE within multiple cortical and subcortical regions. Previous studies indicate that LC neurons projecting to cortical vs. subcortical structures are distributed differentially within the nucleus.

In contrast, basal forebrain-projecting LC neurons were largely distributed uniformly within the LC. These observations suggest that subpopulations of LC neurons that target distinct terminal fields, and thus may represent functionally distinct subpopulations, will nonetheless impact similarly on these three arousal-related basal forebrain regions. This could ensure coordinated regulation of behavioral state with a diversity of LC-modulated state-dependent processes. Moreover, the collateralization of LC neurons across these basal forebrain regions ensures that alterations in LC discharge are conveyed simultaneously to these three regions. Combined, these observations suggest that LC efferents are organized to permit coordinated/simultaneous actions across multiple anatomically distinct, yet functionally related (e.g., arousal-related), basal forebrain fields.

A prominent difference between the SI and both the MSA and MPOR is that the SI is relatively insensitive to the wake-promoting actions of NE and NE agonists (Berridge and O'Neill, 2001). Nonetheless, the SI exerts a robust modulatory influence over forebrain neuronal activity state (Buzsaki et al., 1988; Metherate et al., 1992). Moreover, in vitro, NE depolarizes cholinergic basal forebrain neurons, indicating a neuromodulatory role of NE within the SI (Fort et al., 1995). To date, the behavioral/cognitive functions of NE within the SI remain to be elucidated. However, evidence indicates a role of the SI in state-dependent attentional processes (for review, see Sarter and Bruno, 1999). Thus, NE, released from LC neurons, may act within the SI to modulate state-dependent cognitive processes, such as attention (for review, see Sarter and Bruno, 1999). The high degree of collateralization across the MSA, MPOR, and SI permits the LC to simultaneously modulate behavioral state while modulating SI-dependent behavioral and physiological processes.

ACKNOWLEDGMENTS

The authors thank Dr. Rita Valentino for invaluable advice concerning methodology used in these studies. Additionally, we thank Kate Reis, Carmen Oemig, and Brooke Schmeichel for expert technical assistance.

LITERATURE CITED

Abercrombie M, Johnson ML. 1946. Quantitative histology of Wallerian degeneration I. Nuclear population in rabbit sciatic nerve. J Anat Lond 80:37–50.

Ader JP, Room P, Postema F, Korf J. 1980. Bilaterally diverging axon collaterals and contralateral projections from rat locus coeruleus neurons, demonstrated by fluorescent retrograde double labeling and norepinephrine metabolism. J Neural Transm 49:207–208.

Anderson CH, Shen CL. 1980. Efferents of the medial preoptic area in the guinea pig: an autoradiographic study. Brain Res Bull 5:257–265.

Armstrong DM, Saper CB, Levey AI, Wainer BH, Terry RD. 1983. Distribution of cholinergic neurons in rat brain: demonstrated by the immunocytochemical localization of choline acetyltransferase. J Comp Neurol 216:53–68.

Arnsten AF, Goldman-Rakic PS. 1984. Selective prefrontal cortical projections to the region of the locus coeruleus and raphe nuclei in the rhesus monkey. Brain Res 306:9–18.

Aston-Jones G, Bloom FE. 1981. Activity of norepinephrine-containing locus coeruleus neurons in behaving rats anticipates fluctuations in the sleep-waking cycle. J Neurosci 1:876–886.

Berridge CW, Foote SL. 1991. Effects of locus coeruleus activation on electroencephalographic activity in neocortex and hippocampus. J Neurosci 11:3135–3145.

Berridge CW, Foote SL. 1996. Enhancement of behavioral and electroencephalographic indices of waking following stimulation of noradrenergic beta-receptors within the medial septal region of the basal forebrain. J Neurosci 16:6999–7009.

Berridge CW, O'Neill J. 2001. Differential sensitivity to the wake-promoting actions of norepinephrine within the medial preoptic area and the substantia innominata. Behav Neurosci 115:165–174.

Berridge CW, Waterhouse BD. 2003. The locus coeruleus-noradrenergic system: modulation of behavioral state and state-dependent cognitive processes. Brain Res Brain Res Rev 42:33–84.

Berridge CW, Page ME, Valentino RJ, Foote SL. 1993. Effects of locus coeruleus inactivation on electroencephalographic activity in neocortex and hippocampus. Neuroscience 55:381–393.

Berridge CW, Bolen SJ, Manley MS, Foote SL. 1996. Modulation of forebrain electroencephalographic activity in halothane-anesthetized rat via actions of noradrenergic beta-receptors within the medial septal region. J Neurosci 16:7010–7020.

Berridge CW, O'Neil J, Wifler K. 1999. Amphetamine acts within the medial basal forebrain to initiate and maintain alert waking. Neuroscience 93:885–896.

Berridge CW, Isaac SO, España RA. 2003. Additive wake-promoting actions of medial basal forebrain noradrenergic alpha1- and beta-receptor stimulation. Behav Neurosci 117:350–359.

Buzsaki G, Bickford RG, Ponomareff G, Thal LJ, Mandel R, Gage FH. 1988. Nucleus basalis and thalamic control of neocortical activity in the freely moving rat. J Neurosci 8:4007–4026.

Cape EG, Jones BE. 1998. Differential modulation of high-frequency gamma-electroencephalogram activity and sleep-wake state by noradrenaline and serotonin microinjections into the region of cholinergic basalis neurons. J Neurosci 18:2653–2666.

Castañeyra-Perdomo A, Perez-Delgado MM, Montagnese C, Coen CW. 1992. Brainstem projections to the medial preoptic region containing the luteinizing hormone-releasing hormone perikarya in the rat. An immunohistochemical and retrograde transport study. Neurosci Lett 139:135–139.

Chou TC, Bjorkum AA, Gaus SE, Lu J, Scammell TE, Saper CB. 2002. Afferents to the ventrolateral preoptic nucleus. J Neurosci 22:977–990.

Delfs JM, Zhu Y, Druhan JP, Aston-Jones GS. 1998. Origin of noradrenergic afferents to the shell subregion of the nucleus accumbens: anterograde and retrograde tract-tracing studies in the rat. Brain Res 806: 127–140.

España RA, Baldo BA, Kelley AE, Berridge CW. 2001. Wake-promoting and sleep-suppressing actions of hypocretin (orexin): basal forebrain sites of action. Neuroscience 106:699–715.

Foote SL, Aston-Jones G, Bloom FE. 1980. Impulse activity of locus coeruleus neurons in awake rats and monkeys is a function of sensory stimulation and arousal. Proc Natl Acad Sci U S A 77:3033–3037.

Fort P, Khateb A, Pegna A, Muhlethaler M, Jones BE. 1995. Noradrenergic modulation of cholinergic nucleus basalis neurons demonstrated by in vitro pharmacological and immunohistochemical evidence in the guinea-pig brain. Eur J Neurosci 7:1502–1511.

Grove EA. 1988. Efferent connections of the substantia innominata in the rat. J Comp Neurol 277:347–364.

Haring JH, Davis JN. 1983. Topography of locus ceruleus neurons projecting to the area dentata. Exp Neurol 79:785–800.

Hobson JA, McCarley RW, Wyzinski PW. 1975. Sleep cycle oscillation: reciprocal discharge by two brainstem neuronal groups. Science 189: 55–58.

Jones BE, Cuello AC. 1989. Afferents to the basal forebrain cholinergic cell area from pontomesencephalic—catecholamine, serotonin, and acetylcholine—neurons. Neuroscience 31:37–61.

Jones BE, Moore RY. 1977. Ascending projections of the locus coeruleus in the rat. II. Autoradiographic study. Brain Res 127:25–53.

Krayniak PF, Meibach RC, Siegel A. 1981. Origin of brain stem and temporal cortical afferent fibers to the septal region in the squirrel monkey. Exp Neurol 72:113–121.

Kumar VM, Datta S, Chhina GS, Singh B. 1986. Alpha adrenergic system in medial preoptic area involved in sleep-wakefulness in rats. Brain Res Bull 16:463–468.

Lindvall O, Bjorklund A. 1983. Dopamine and norepinephrine containing neuron systems. In: Emson, PC, editor. Chemical neuroanatomy. New York: Raven Press. p 229–255.

Loughlin SE, Foote SL, Bloom FE. 1986. Efferent projections of nucleus locus coeruleus: topographic organization of cells of origin demonstrated by three-dimensional reconstruction. Neuroscience 18:291–306.

Loy R, Koziell DA, Lindsey JD, Moore RY. 1980. Noradrenergic innervation of the adult rat hippocampal formation. J Comp Neurol 189:699–710.

Mallick BN, Alam MN. 1992. Different types of norepinephrinergic receptors are involved in preoptic area mediated independent modulation of sleep-wakefulness and body temperature. Brain Res 591:8–19.

Mesulam MM, Mufson EJ, Wainer BH, Levey AI. 1983. Central cholinergic pathways in the rat: an overview based on an alternative nomenclature (Ch1–Ch6). Neuroscience 10:1185–1201.

Metherate R, Cox CL, Ashe JH. 1992. Cellular bases of neocortical activation: modulation of neural oscillations by the nucleus basalis and endogenous acetylcholine. J Neurosci 12:4701–4711.

Moore RY. 1978. Catecholamine innervation of the basal forebrain. I. The septal area. J Comp Neurol 177:665–684.

Paxinos G, Carrive P, Wang H, Wang P. 1999. Chemoarchitectonic atlas of the rat brainstem. San Diego: Academic Press.

Pieribone VA, Aston-Jones G. 1988. The iontophoretic application of Fluoro-Gold for the study of afferents to deep brain nuclei. Brain Res 475:259–271.

Saper CB, Reis DJ, Joh T. 1983. Medullary catecholamine inputs to the anteroventral third ventricular cardiovascular regulatory region in the rat. Neurosci Let 42:285–291.

Sarter M, Bruno JP. 1999. Abnormal regulation of corticopetal cholinergic neurons and impaired information processing in neuropsychiatric disorders. Trends Neurosci 22:67–74.

Segal M, Landis SC. 1974. Afferents to the septal area of the rat studied with the method of retrograde axonal transport of horseradish peroxidase. Brain Res 82:263–268.

Semba K, Reiner PB, McGeer EG, Fibiger HC. 1988. Brainstem afferents to the magnocellular basal forebrain studied by axonal transport, immunohistochemistry, and electrophysiology in the rat. J Comp Neurol 267:433–453.

Simpson KL, Altman DW, Wang L, Kirifides ML, Lin RC, Waterhouse BD. 1997. Lateralization and functional organization of the locus coeruleus projection to the trigeminal somatosensory pathway in rat. J Comp Neurol 385:135–147.

Swanson LW. 1998. Brain maps: structure of the rat brain. Amsterdam: Elsevier Science Publishers.

Swanson LW, Cowan WM. 1979. The connections of the septal region in the rat. J Comp Neurol 186:621–655.

Thakkar MM, Ramesh V, Strecker RE, McCarley RW. 2001. Microdialysis perfusion of orexin-A in the basal forebrain increases wakefulness in freely behaving rats. Arch Ital Biol 139:313–328.

Tucker DC, Saper CB, Ruggiero DA, Reis DJ. 1987. Organization of central adrenergic pathways: I. Relationships of ventrolateral medullary projections to the hypothalamus and spinal cord. J Comp Neurol 259:591–603.

Valentino RJ, Foote SL, Aston-Jones G. 1983. Corticotropin-releasing factor activates noradrenergic neurons of the locus coeruleus. Brain Res 270:363–367.

Valentino RJ, Page ME, Luppi PH, Zhu Y, Van Bockstaele E, Aston-Jones G. 1994. Evidence for widespread afferents to Barrington's nucleus, a brainstem region rich in corticotropin-releasing hormone neurons. Neuroscience 62:125–143.

Van Bockstaele EJ, Colago EE, Valentino RJ. 1998. Amygdaloid corticotropin-releasing factor targets locus coeruleus dendrites: substrate for the co-ordination of emotional and cognitive limbs of the stress response. J Neuroendocrinol 10:743–757.

Vertes RP. 1988. Brainstem afferents to the basal forebrain in the rat. Neuroscience 24:907–935.

Waterhouse BD, Lin CS, Burne RA, Woodward DJ. 1983. The distribution of neocortical projection neurons in the locus coeruleus. J Comp Neurol 217:418–431.

Waterhouse BD, Border B, Wahl L, Mihailoff GA. 1993. Topographic organization of rat locus coeruleus and dorsal raphe nuclei: distribution of cells projecting to visual system structures. J Comp Neurol 336:345–361.

Zaborsky L. 1989. Afferent connections of the forebrain cholinergic projection neurons, with special reference to monoaminergic and peptidergic fibers. In: Frotscher M, Misgel U, editors. Central cholinergic synaptic transmission. Basel: Birkhauser. p 12–32.